Possibility of observation of hidden-bottom pentaquark resonances in bottomonium photoproduction on protons and nuclei near threshold

E. Ya. Paryev[1,2;1)]

[1]Institute for Nuclear Research, Russian Academy of Sciences, Moscow 117312, Russia
[2]Institute for Theoretical and Experimental Physics, Moscow 117218, Russia

Abstract: We study the $\Upsilon(1S)$ meson photoproduction on protons and nuclei at near-threshold center-of-mass energies below 11.4 GeV (or at the corresponding photon laboratory energies E_γ below 68.8 GeV). We calculate the absolute excitation functions for the nonresonant and resonant photoproduction of $\Upsilon(1S)$ mesons off protons at incident photon laboratory energies of 63-68 GeV by considering direct ($\gamma p \to \Upsilon(1S)p$) and two-step ($\gamma p \to P_b^+(11080) \to \Upsilon(1S)p$, $\gamma p \to P_b^+(11125) \to \Upsilon(1S)p$, $\gamma p \to P_b^+(11130) \to \Upsilon(1S)p$) $\Upsilon(1S)$ production channels within different scenarios for the nonresonant total cross section of the elementary reaction $\gamma p \to \Upsilon(1S)p$ and for branching ratios of the decays $P_b^+(11080) \to \Upsilon(1S)p$, $P_b^+(11125) \to \Upsilon(1S)p$, and $P_b^+(11130) \to \Upsilon(1S)p$. We also calculate an analogous function for the photoproduction of $\Upsilon(1S)$ mesons on the ^{12}C and ^{208}Pb target nuclei in the near-threshold center-of-mass beam energy region of 9.0-11.4 GeV by considering the respective incoherent direct ($\gamma N \to \Upsilon(1S)N$) and two-step ($\gamma p \to P_b^+(11080) \to \Upsilon(1S)p, \gamma p \to P_b^+(11125) \to \Upsilon(1S)p, \gamma p \to P_b^+(11130) \to \Upsilon(1S)p$ and $\gamma n \to P_b^0(11080) \to \Upsilon(1S)n$, $\gamma n \to P_b^0(11125) \to \Upsilon(1S)n$, $\gamma n \to P_b^0(11130) \to \Upsilon(1S)n$) $\Upsilon(1S)$) production processes using a nuclear spectral function approach. We demonstrate that a detailed scan of the $\Upsilon(1S)$ total photoproduction cross section on proton and nuclear targets in the near-threshold energy region in future high-precision experiments at the proposed high-luminosity electron-ion colliders EIC and EicC in the US and China should provide a definite result for or against the existence of the nonstrange hidden-bottom pentaquark states P_{bi}^+ and P_{bi}^0 (i=1, 2, 3) as well as clarify their decay rates.

Keywords: photon-nucleus reactions, bottomonium production, hidden-bottom pentaquarks

DOI: 10.1088/1674-1137/aba5f8

1 Introduction

In a recent publication [1], the role of the new narrow hidden-charm pentaquark states $P_c^+(4312)$, $P_c^+(4440)$, and $P_c^+(4457)$, discovered by the LHCb Collaboration in the $J/\psi p$ invariant mass spectrum of the $\Lambda_b^0 \to K^-(J/\psi p)$ decays [2], in near-threshold J/ψ photoproduction on nuclei has been studied in the framework of the nuclear spectral function approach by considering both the direct nonresonant ($\gamma N \to J/\psi N$) and two-step resonant ($\gamma p \to P_c^+(4312)$, $P_c^+(4312) \to J/\psi p$; $\gamma p \to P_c^+(4440)$, $P_c^+(4440) \to J/\psi p$; and $\gamma p \to P_c^+(4457)$, $P_c^+(4457) \to J/\psi p$) J/ψ elementary production processes. It should be noted that such role of initially claimed [3] by the LHCb Collaboration pentaquark resonance $P_c^+(4450)$ in J/ψ photoproduction on nuclei at near-threshold incident photon energies of 5–11 GeV has been investigated in our previous work [4]. In the calculations, the new experimental data for the total and differential cross sections of the exclusive reaction $\gamma p \to J/\psi p$ in the threshold energy region have been incorporated from the GlueX experiment [5]. The model-dependent upper limits on the branching ratios of the $P_c^+(4312) \to J/\psi p$, $P_c^+(4440) \to J/\psi p$, and $P_c^+(4457) \to J/\psi p$ decays, set in this experiment, have been considered in them as well.

The quark structure of the abovementioned pentaquarks is $|P_c^+> = |uudc\bar{c}>$, i.e., they are composed of three light quarks u, u, d and a charm-anticharm pair $c\bar{c}$. In a molecular scenario, owing to the closeness of the observed $P_c^+(4312)$, $P_c^+(4440)$, and $P_c^+(4457)$ masses to the $\Sigma_c^+\bar{D}^0$ and $\Sigma_c^+\bar{D}^{*0}$ thresholds, the $P_c^+(4312)$ resonance can be, in particular, considered as an S-wave $\Sigma_c^+\bar{D}^0$ bound state, whereas the $P_c^+(4440)$ and $P_c^+(4457)$ resonances can

Received 18 March 2020, Published online 18 August 2020

1) E-mail: paryev@inr.ru

be considered as S-wave $\Sigma_c^+\bar{D}^{*0}$ bound molecular states [6-18]. The existence of molecular type hidden-charm pentaquark resonances has been predicted before the LHCb observation [2, 3] in some earlier papers (see, for example, [19-25]). It is natural to extend this picture to the bottom sector, replacing the $c\bar{c}$ pair with the bottom-antibottom $b\bar{b}$ pair, nonstrange $D(D^*)$ mesons with the $B(B^*)$ ones, and charmed baryons with the bottom ones. Based on the classification of hidden-charm pentaquarks composed of a single charm baryon and $D(D^*)$ mesons, such an extension has been performed in Ref. [26] using the hadronic molecular approach. Therefore, the classification of hidden-bottom pentaquarks composed of a single bottom baryon and $B(B^*)$ mesons has been presented here. Accordingly, the charged hidden-bottom partners $P_b^+(11080)$, $P_b^+(11125)$, and $P_b^+(11130)$ of the observed hidden-charm pentaquarks $P_c^+(4312)$, $P_c^+(4440)$, and $P_c^+(4457)$, having the quark structure $|P_b^+>=|uudb\bar{b}>$, were predicted to exist, with masses 11080, 11125, and 11130 MeV, respectively. Moreover, the predictions for the neutral hidden-bottom counterparts $P_b^0(11080)$, $P_b^0(11125)$ and $P_b^0(11130)$ of the unobserved hidden-charm states $P_c^0(4312)$, $P_c^0(4440)$, and $P_c^0(4457)$ with the quark structure $|P_b^0>=|uddb\bar{b}>$ were provided in [26] as well. These new exotic heavy pentaquarks can decay into the $\Upsilon(1S)p$ and $\Upsilon(1S)n$ final states. They can be searched for through a scan of the cross section[1)] of the exclusive reaction $\gamma p\to\Upsilon(1S)p$ from a threshold of 10.4 GeV and up to the photon γp c.m.s. energy W = 11.4 GeV (cf. [27]).

Therefore, it is interesting to extend the study of Ref. [1] to the consideration of bottomonium $\Upsilon(1S)$ photoproduction on protons and nuclei near the threshold to shed light on the possibility of observing such hidden-bottom pentaquarks in this photoproduction in future high-precision experiments at the proposed high-luminosity electron-ion colliders EIC [28-30] and EicC [31, 32] in the US and China. This is the main purpose of the present study. We briefly recapitulate the main assumptions of the model [1] and describe, where necessary, the corresponding extensions. Additionally, we present the predictions obtained within this expanded model for the $\Upsilon(1S)$ excitation functions in γp as well as γ^{12}C and γ^{208}Pb collisions at near-threshold incident energies. These predictions may serve as guidance for future dedicated experiments at the abovementioned colliders.

2 Model

2.1 Direct processes of nonresonant $\Upsilon(1S)$ photoproduction on nuclei

An incident photon can produce a $\Upsilon(1S)$ meson directly in the first inelastic γN collision. As we are interested in near-threshold center-of-mass photon beam energies $\sqrt{s}$ below 11.4 GeV, corresponding to the laboratory incident photon energies E_γ below 68.8 GeV or excess energies $\epsilon_{\Upsilon(1S)N}$ above the $\Upsilon(1S)N$ threshold $\sqrt{s_{\rm th}}=m_{\Upsilon(1S)}+m_N=10.4$ GeV ($m_{\Upsilon(1S)}$ and m_N are the lowest-lying bottomonium and nucleon bare masses, respectively), $\epsilon_{\Upsilon(1S)N}=\sqrt{s}-\sqrt{s_{\rm th}}\leqslant 1.0$ GeV, we have considered the following direct nonresonant elementary $\Upsilon(1S)$ production processes, which have the lowest free production threshold:[2)]

$$\gamma+p\to\Upsilon(1S)+p, \tag{1}$$

$$\gamma+n\to\Upsilon(1S)+n. \tag{2}$$

In line with [33], we neglect the modification of the outgoing $\Upsilon(1S)$ mass in the nuclear matter. Furthermore, we ignore the medium modification of the secondary high-momentum nucleon mass in the present work.

Disregarding the absorption of incident photons in the energy range of interest and describing the $\Upsilon(1S)$ meson absorption in the nuclear medium using the absorption cross section $\sigma_{\Upsilon(1S)N}$, we can represent the total cross section for the production of $\Upsilon(1S)$ mesons off nuclei in the direct nonresonant channels (1) and (2) of their production off target nucleons in the following form [4]:

$$\sigma^{\rm (dir)}_{\gamma A\to\Upsilon(1S)X}(E_\gamma)=I_V[A,\sigma_{\Upsilon(1S)N}]\left\langle\sigma_{\gamma p\to\Upsilon(1S)p}(E_\gamma)\right\rangle_A, \tag{3}$$

where

$$I_V[A,\sigma]=2\pi A\int_0^R r_\perp {\rm d}r_\perp\int_{-\sqrt{R^2-r_\perp^2}}^{\sqrt{R^2-r_\perp^2}}{\rm d}z\rho(\sqrt{r_\perp^2+z^2})\times\exp\left[-A\sigma\int_z^{\sqrt{R^2-r_\perp^2}}\rho(\sqrt{r_\perp^2+x^2}){\rm d}x\right], \tag{4}$$

$$\left\langle\sigma_{\gamma p\to\Upsilon(1S)p}(E_\gamma)\right\rangle_A=\int\!\!\int P_A(\mathbf{p}_t,E){\rm d}\mathbf{p}_t{\rm d}E\sigma_{\gamma p\to\Upsilon(1S)p}(\sqrt{s_{\Upsilon(1S)}}) \tag{5}$$

and

$$s_{\Upsilon(1S)}=(E_\gamma+E_t)^2-(\mathbf{p}_\gamma+\mathbf{p}_t)^2, \tag{6}$$

$$E_t=M_A-\sqrt{(-\mathbf{p}_t)^2+(M_A-m_N+E)^2}. \tag{7}$$

Here, $\sigma_{\gamma p\to\Upsilon(1S)p}(\sqrt{s_{\Upsilon(1S)}})$ is the "in-medium" total cross section for the production of $\Upsilon(1S)$ in reaction (1)[3)] at the "in-medium" γp center-of-mass energy $\sqrt{s_{\Upsilon(1S)}}$; $\rho(\mathbf{r})$ and $P_A(\mathbf{p}_t,E)$ are the local nucleon density and the nuclear spectral function of target nucleus A normalized

1) They should appear as structures at W = 11080, 11125 and 11130 MeV or at laboratory photon energies E_γ = 64.952, 65.484 and 65.544 GeV in this cross section.

2) We can ignore in the energy domain of our interest the contribution to the $\Upsilon(1S)$ yield from the excited bottomonium states $\Upsilon(2S)$, $\Upsilon(3S)$ and $\chi_{\rm b}(1P)$, $\chi_{\rm b}(2P)$ mesons feed-down due to larger their production thresholds in γN collisions.

3) In equation (3) it is supposed that the $\Upsilon(1S)$ meson production cross sections in γp and γn interactions are the same.

to unity, (the concrete information about these quantities, used in our subsequent calculations, is given in [34-36]); $\mathbf{p}_t$ and E are the internal momentum and binding energy, respectively, of the struck target nucleon just before the collision; A is the number of nucleons in the target nucleus, M_A and R are its mass and radius, respectively; and $\mathbf{p}_\gamma$ and E_γ are the laboratory momentum and energy, respectively, of the initial photon. Motivated by the fact that the nuclear medium suppresses $\Upsilon(1S)$ production as much as J/ψ production, we employ the same value of 3.5 mb for the $\Upsilon(1S)$–nucleon absorption cross section $\sigma_{\Upsilon(1S)N}$ in our calculations, as was adopted in Ref. [4] for the J/ψ–nucleon absorption cross section $\sigma_{J/\psi N}$ (compare [37-39]).

As mentioned earlier [4], we suggest that the "in-medium" cross section $\sigma_{\gamma p\to\Upsilon(1S)p}(\sqrt{s_{\Upsilon(1S)}})$ for $\Upsilon(1S)$ production in process (1) is equivalent to the vacuum cross section $\sigma_{\gamma p\to\Upsilon(1S)p}(\sqrt{s})$, in which the vacuum center-of-mass energy squared s, presented by the formula

$$s = W^2 = (E_\gamma + m_N)^2 - \mathbf{p}_\gamma^2, \tag{8}$$

is replaced by the in-medium expression (6). The latter cross section has been determined experimentally both earlier [40-42] and recently [43, 44] only at high photon-proton center-of-mass energies $W = \sqrt{s} > 60$ GeV (see Fig. 2 below). Furthermore, thus far, the experimental data on $\Upsilon(1S)$ production in the channel $\gamma p \to \Upsilon(1S)p$ have not been not available in the threshold energy region $W \leqslant 11.4$ GeV, where the masses of the predicted [26] P_b states are concentrated and where they can be observed [27] in the γp reactions.

The total cross section of this channel can be evaluated using the following indirect route. An analysis of the data on the production of $\Upsilon(1S)$ and J/ψ mesons in γp collisions in the kinematic range of $80 < W < 160$GeV, conducted by the ZEUS Collaboration at HERA [40], yielded the following ratio of $\Upsilon(1S)$ to J/ψ photoproduction cross sections in this range:

$$\sigma_{\gamma p\to\Upsilon(1S)p}(W)/\sigma_{\gamma p\to J/\psi p}(W) \approx 5\cdot 10^{-3}. \tag{9}$$

Considering the commonality in the J/ψ and $\Upsilon(1S)$ production in γp interactions [45], we assume that in the threshold region $W \leqslant 11.4$GeV, the ratio of the total cross sections of the reactions $\gamma p \to \Upsilon(1S)p$ and $\gamma p \to J/\psi p$ is the same as that expressed by Eq. (9) derived at the same high γp c.m.s. energies. However, in this ratio, the former and latter cross sections are calculated, respectively, at the collisional energies $\sqrt{s}$ and $\sqrt{\tilde{s}}$, which correspond to the same excess energies $\epsilon_{\Upsilon(1S)N}$ and $\epsilon_{J/\psi N}$ above the $\Upsilon(1S)N$ and $J/\psi N$ thresholds, respectively, namely,

$$\sigma_{\gamma p\to\Upsilon(1S)p}(\sqrt{s})/\sigma_{\gamma p\to J/\psi p}(\sqrt{\tilde{s}}) \approx 5\cdot 10^{-3}, \tag{10}$$

where, according to the preceding discussion, the center-of-mass energies $\sqrt{s}$ and $\sqrt{\tilde{s}}$ are linked by the relation

$$\epsilon_{J/\psi N} = \sqrt{\tilde{s}} - \sqrt{\tilde{s}_{\rm th}} = \epsilon_{\Upsilon(1S)N} = \sqrt{s} - \sqrt{s_{\rm th}}. \tag{11}$$

Here, $\sqrt{\tilde{s}_{\rm th}} = m_{J/\psi} + m_N$ ($m_{J/\psi}$ is the bare J/ψ meson mass). Thus, we have

$$\sqrt{\tilde{s}} = \sqrt{s} - \sqrt{s_{\rm th}} + \sqrt{\tilde{s}_{\rm th}} = \sqrt{s} - m_{\Upsilon(1S)} + m_{J/\psi}. \tag{12}$$

Evidently, at high energies, $\sqrt{s} \gg \sqrt{s_{\rm th}}$, $\sqrt{\tilde{s}} \approx \sqrt{s}$, and the expression (10) transforms into Eq. (9). At low incident photon energies, $\sqrt{s} \leqslant 11.4$ GeV, of interest, the c.m.s. energy $\sqrt{\tilde{s}} \leqslant 5.04$ GeV. The latter corresponds to the laboratory photon energy domain $\leqslant 13.05$ GeV. For the free total cross section $\sigma_{\gamma p\to J/\psi p}(\sqrt{\tilde{s}})$ in this domain, we have adopted the following expression [1], based on the predictions of the two-gluon and three-gluon exchange model [46] near the threshold:

$$\sigma_{\gamma p\to J/\psi p}(\sqrt{\tilde{s}}) = \sigma_{2g}(\sqrt{\tilde{s}}) + \sigma_{3g}(\sqrt{\tilde{s}}), \tag{13}$$

where

$$\sigma_{2g}(\sqrt{\tilde{s}}) = a_{2g}(1-x)^2\left[\frac{e^{bt^+} - e^{bt^-}}{b}\right], \tag{14}$$

$$\sigma_{3g}(\sqrt{\tilde{s}}) = a_{3g}(1-x)^0\left[\frac{e^{bt^+} - e^{bt^-}}{b}\right], \tag{15}$$

and

$$x = (\tilde{s}_{\rm th} - m_N^2)/(\tilde{s} - m_N^2). \tag{16}$$

Here, t^+ and t^- are, respectively, the maximal and minimal values of the squared four-momentum transfer t between the incident photon and the outgoing J/ψ meson. These values correspond to the value of t at which J/ψ is produced at angles of 0° and 180° in γp c.m.s., respectively. These can be readily expressed in terms of the total energies and momenta of the initial photon and the J/ψ meson, E^*_γ, p^*_γ, and $E^*_{J/\psi}, p^*_{J/\psi}$ in this system as follows:

$$t^\pm = m^2_{J/\psi} - 2E^*_\gamma(m_N^2)E^*_{J/\psi}(m_{J/\psi}) \pm 2p^*_\gamma(m_N^2)p^*_{J/\psi}(m_{J/\psi}), \tag{17}$$

where

$$p^*_\gamma(m_N^2) = \frac{1}{2\sqrt{\tilde{s}}}\lambda(\tilde{s}, 0, m_N^2), \tag{18}$$

$$p^*_{J/\psi}(m_{J/\psi}) = \frac{1}{2\sqrt{\tilde{s}}}\lambda(\tilde{s}, m^2_{J/\psi}, m_N^2), \tag{19}$$

and

$$E^*_\gamma(m_N^2) = p^*_\gamma(m_N^2),\ \ E^*_{J/\psi}(m_{J/\psi}) = \sqrt{m^2_{J/\psi} + [p^*_{J/\psi}(m_{J/\psi})]^2}; \tag{20}$$

$$\lambda(x,y,z) = \sqrt{\left[x - (\sqrt{y} + \sqrt{z})^2\right]\left[x - (\sqrt{y} - \sqrt{z})^2\right]}. \tag{21}$$

The parameter b in Eqs. (14) and (15) is an exponential t-slope of the differential cross section of the reaction $\gamma p \to J/\psi p$ near the threshold [46]. According to [5], $b \approx 1.67$ GeV^{-2}. We employ this value in our calculations. The normalization coefficients a_{2g} and a_{3g} were determ-

ined in [1] as $a_{2g} = 44.780$ nb/GeV^2 and $a_{3g} = 2.816$ nb/GeV^2, assuming that the incoherent sum (13) saturates at the total experimental cross section of the reaction $\gamma p \to J/\psi p$ measured at GlueX [5] at photon energies of approximately 8.38 and 11.62 GeV.

The results of the calculations performed using Eqs. (10)–(20) of the nonresonant total cross section of the reaction $\gamma p \to \Upsilon(1S)p$ at "low" energies are depicted in Fig. 1 (solid curve). In this figure, we also depict the predictions made using the dipole Pomeron model [27] (dashed curve)[1] and from the recently proposed parametrization [45]

$$\sigma_{\gamma p\to\Upsilon(1S)p}(\sqrt{s}) = 33.9(1-x_\Upsilon)^{1.8}\ \text{[pb]}, \tag{22}$$

where x_Υ is defined as

$$x_\Upsilon = (s_{\rm th}-m_N^2)/(s-m_N^2) \tag{23}$$

(dotted-dashed curve). The results from the extrapolation of the fit [47]

$$\sigma_{\gamma p\to\Upsilon(1S)p}(\sqrt{s}) = 0.7(\sqrt{s})^{1.18}\ \text{[pb]} \tag{24}$$

of the high-energy data [42] (see Fig. 2 where also the data from other high-energy experiments [40, 41, 43] are given) to the threshold energies of interest are depicted in Fig. 1 as well (dotted curve). In particular, it is seen that at photon energies of approximately 11 GeV, our parametrization (10)-(20) is close to the results obtained from the high-energy fit (24), and it is considerably greater (by factors of approximately 5 and 15, respectively) than the results obtained from the dipole Pomeron model [27] and

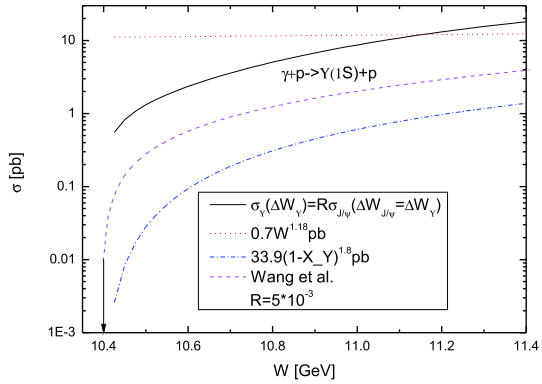

Fig. 1. (color online) Nonresonant total cross section for reaction $\gamma p \to \Upsilon(1S)p$ as a function of the center-of-mass energy $W = \sqrt{s}$ of photon–proton collisions. Solid, dashed, dotted-dashed and dotted curves represent calculations performed using Eqs. (10)-(20), within the dipole Pomeron model [27], using Eqs. (22) and (24), respectively. The arrow indicates the center-of-mass threshold energy for direct $\Upsilon(1S)$ photoproduction on a free target proton being at rest.

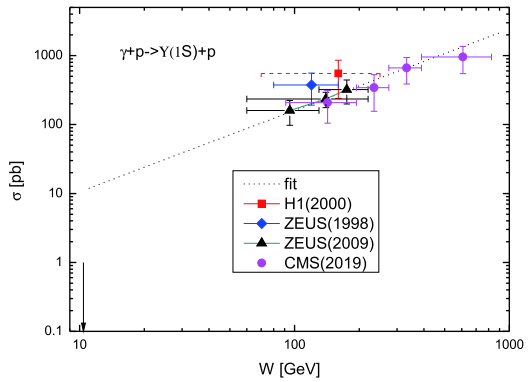

Fig. 2. (color online) Nonresonant total cross section for reaction $\gamma p \to \Upsilon(1S)p$ as a function of the center-of-mass energy $W = \sqrt{s}$ of photon–proton collisions. The dotted curve represents calculation using (24). Experimental data are from Refs. [40-43]. The arrow indicates the center-of-mass threshold energy for direct $\Upsilon(1S)$ photoproduction on a free target proton at rest.

the parametrization (22). Therefore, the use of the two parametrizations (10)-(20) and (22) in our subsequent calculations yields reasonable bounds for the elastic background under the pentaquark peaks. When these bounds are employed in the calculations of the nonresonant $\Upsilon(1S)$ photoproduction off nuclei presented below, then, in line with the preceding discussion, instead of the vacuum quantity s, appearing in Eqs. (10)-(12) and (23), one must adopt its in-medium expression (6), in which the laboratory incident photon energy E_γ is expressed through the given free space center-of-mass energy W as $E_\gamma = (W^2-m_N^2)/(2m_N)$. Furthermore, instead of using the quantity m_N^2 in Eq. (18), we should employ the difference $E_t^2 - p_t^2$.

2.2 Two-step processes of resonant $\Upsilon(1S)$ photoproduction on nuclei

At photon center-of-mass energies $\leqslant 11.4$ GeV, an incident photon can produce nonstrange charged $P_b^+(11080)$, $P_b^+(11125)$, and $P_b^+(11130)$ and neutral $P_b^0(11080)$, $P_b^0(11125)$, and $P_b^0(11130)$ resonances with the pole masses $M_{b1} = 11080$ MeV, $M_{b2} = 11125$ MeV, and $M_{b3} = 11130$ MeV, respectively, as predicted in Ref. [26] based on the observed [2] three P_c^+ states, in the first inelastic collision with intranuclear protons and neutrons:[2]

$$\begin{aligned}&\gamma + p \to P_b^+(11080),\\ &\gamma + p \to P_b^+(11125),\\ &\gamma + p \to P_b^+(11130);\end{aligned} \tag{25}$$

1) The author thanks X.-Y. Wang for sending these predictions to him.

2) We recall that the threshold (resonant) energies $E_\gamma^{\rm R1}$, $E_\gamma^{\rm R2}$, $E_\gamma^{\rm R3}$ for the photoproduction of $P_b^+(11080)$, $P_b^+(11125)$, $P_b^+(11130)$ and $P_b^0(11080)$, $P_b^0(11125)$, $P_b^0(11130)$ resonances on a free target protons and neutrons being at rest are $E_\gamma^{\rm R1} = 64.952$ GeV, $E_\gamma^{\rm R2} = 65.484$ GeV, $E_\gamma^{\rm R3} = 65.544$ GeV and $E_\gamma^{\rm R1} = 64.863$ GeV, $E_\gamma^{\rm R2} = 65.395$ GeV, $E_\gamma^{\rm R3} = 65.454$ GeV, respectively.

$$\gamma+n\to P_b^0(11080),$$
$$\gamma+n\to P_b^0(11125),$$
$$\gamma+n\to P_b^0(11130). \quad (26)$$

Furthermore, the produced intermediate pentaquarks can decay into the final states $\Upsilon(1S)p$ and $\Upsilon(1S)n$:

$$P_b^+(11080)\to\Upsilon(1S)+p,$$
$$P_b^+(11125)\to\Upsilon(1S)+p,$$
$$P_b^+(11130)\to\Upsilon(1S)+p; \quad (27)$$

$$P_b^0(11080)\to\Upsilon(1S)+n,$$
$$P_b^0(11125)\to\Upsilon(1S)+n,$$
$$P_b^0(11130)\to\Upsilon(1S)+n. \quad (28)$$

As the P_{bi}^+ and P_{bi}^0 states have not been observed experimentally until now, neither their total decay widths Γ_{bi}, branching ratios $Br[P_{bi}^+\to\Upsilon(1S)p]$ and $Br[P_{bi}^0\to\Upsilon(1S)n]$ [1)] of decays (27) and (28), nor spin-parity quantum numbers are known in a model-independent way at present. Therefore, to estimate the $\Upsilon(1S)$ production cross section from the production/decay chains (25)-(28), one must rely on the theoretical predictions as well as the similarity of the basic features of the decay properties of the $qqqb\bar{b}$ and $qqqc\bar{c}$ systems (with $q=u$ or d). Thus, the results for the decay rates of the modes (27) and (28) are expressed in Ref. [26] in terms of the model parameter Λ, which should be constrained from the future experiments. The existence of the hidden-bottom pentaquark resonances with masses of approximately 11 GeV and total decay widths ranging from a few to 45 MeV has also been predicted in Refs. [48-50]. Therefore, it is natural to assume, analogously to [47], for the P_{bi}^+ and P_{bi}^0 states the same total widths Γ_{bi} as for their hidden-charm partners $P_c^+(4312)$, $P_c^+(4440)$, and $P_c^+(4457)$, i.e., $\Gamma_{b1}=9.8$ MeV, $\Gamma_{b2}=20.6$ MeV, and $\Gamma_{b3}=6.4$ MeV [2]. In addition, for all branching ratios $Br[P_{bi}^+\to\Upsilon(1S)p]$ and $Br[P_{bi}^0\to\Upsilon(1S)n]$ of the decays (27) and (28), the same [47] three main options, $Br[P_{bi}^+\to\Upsilon(1S)p]=1\%$, 2%, and 3% and $Br[P_{bi}^0\to\Upsilon(1S)n]=1\%$, 2%, and 3%, as those used in Ref. [1] for the $P_{ci}^+\to J/\psi p$ decays are adopted in our study. In addition, to determine the size of the impact of the branching fractions $Br[P_{bi}^+\to\Upsilon(1S)p]$ and $Br[P_{bi}^0\to\Upsilon(1S)n]$ on the resonant $\Upsilon(1S)$ yields in $\gamma p\to\Upsilon(1S)p$, $\gamma^{12}\mathrm{C}\to\Upsilon(1S)X$, and $\gamma^{208}\mathrm{Pb}\to\Upsilon(1S)X$ reactions, we also calculate these yields assuming that all these branching fractions are equal to 5% and 10% as well.

According to [1], a majority of the P_{bi}^+ and P_{bi}^0 ($i=1$, 2, 3) resonances, having vacuum total decay widths in their rest frames $\Gamma_{b1}=9.8$ MeV, $\Gamma_{b2}=20.6$ MeV, and $\Gamma_{b3}=6.4$ MeV, respectively, decay to $\Upsilon(1S)p$ and $\Upsilon(1S)n$ out of the target nuclei of interest. As in [1], for the P_{ci}^+ states, their free spectral functions are assumed to be described by the non-relativistic Breit-Wigner distributions:

$$S_{bi}^+(\sqrt{s},\Gamma_{bi})=S_{bi}^0(\sqrt{s},\Gamma_{bi})=\frac{1}{2\pi}\frac{\Gamma_{bi}}{(\sqrt{s}-M_{bi})^2+\Gamma_{bi}^2/4},\ i=1,2,3; \quad (29)$$

where $\sqrt{s}$ is the total γN c.m.s. energy defined by Eq. (8). It should be pointed out that when the excitation functions for the production of P_{bi}^+ and P_{bi}^0 ($i=1$, 2, 3) resonances in reactions (25) and (26) on ^{12}C and ^{208}Pb targets in the "free" P_{bi}^+ and P_{bi}^0 spectral function scenario are calculated, this energy should be considered in the form of Eq. (6). The spectral functions S_{bi}^+ and S_{bi}^0 correspond to P_{bi}^+ and P_{bi}^0, respectively. In line with [1], we assume that the in-medium spectral functions $S_{bi}^+(\sqrt{s},\Gamma_{\mathrm{med}}^{bi})$ and $S_{bi}^0(\sqrt{s},\Gamma_{\mathrm{med}}^{bi})$ are also described by the Breit-Wigner formula (29) with the total in-medium widths $\Gamma_{\mathrm{med}}^{bi}$ ($i=1$, 2, 3) in their rest frames, obtained as a sum of the vacuum decay widths Γ_{bi} and averaged over the local nucleon density $\rho_N(\mathbf{r})$ collisional widths $\langle\Gamma_{\mathrm{coll},bi}\rangle$ appearing because of the P_{bi}^+N and P_{bi}^0N inelastic collisions:

$$\Gamma_{\mathrm{med}}^{bi}=\Gamma_{bi}+\langle\Gamma_{\mathrm{coll},bi}\rangle,\ i=1,2,3. \quad (30)$$

According to [4], the average collisional width $\langle\Gamma_{\mathrm{coll},bi}\rangle$ has the form

$$\langle\Gamma_{\mathrm{coll},bi}\rangle=\gamma_c v_c\sigma_{P_{bi}N}\langle\rho_N\rangle. \quad (31)$$

Here, $\sigma_{P_{bi}N}$ is the P_{bi}^+, P_{bi}^0–nucleon inelastic cross section, and the Lorentz γ-factor γ_c and the velocity v_c of the resonances P_{bi}^+, P_{bi}^0 in the nuclear rest frame are determined as follows:

$$\gamma_c=\frac{(E_\gamma+E_t)}{\sqrt{s}},\quad v_c=\frac{|\mathbf{p}_\gamma+\mathbf{p}_t|}{(E_\gamma+E_t)}. \quad (32)$$

Taking into account the quark contents of the hidden-charm and hidden-bottom pentaquarks as well as the fact that the nuclear medium suppresses $\Upsilon(1S)$ production as much as J/ψ production, we will employ in the following calculations for the absorption cross section $\sigma_{P_{bi}N}$ for each P_{bi}^+ and P_{bi}^0 ($i=1$, 2, 3) the same value of 33.5 mb as was adopted in Ref. [1] for the P_{ci}^+–nucleon absorption cross section. Within the hadronic molecular scenario of P_{bi}^+ and P_{bi}^0 states [26, 47-53] in which their spins-parities are $J^P=(1/2)^-$ for P_{b1}^+ and P_{b1}^0, $J^P=(1/2)^-$ for P_{b2}^+ and P_{b2}^0, and $J^P=(3/2)^-$ for P_{b3}^+ and P_{b3}^0 [26, 27], the free Breit-Wigner total cross sections for their production in reactions (25) and (26) can be described based on the spectral functions (29) and the known branching fractions $Br[P_{bi}^+\to\gamma p]$ and $Br[P_{bi}^0\to\gamma n]$ ($i=1$, 2, 3) as fol-

1) Here, $i=1$, 2, 3. P_{b1}^+, P_{b2}^+, P_{b3}^+ and P_{b1}^0, P_{b2}^0, P_{b3}^0 stand for $P_b^+(11080)$, $P_b^+(11125)$, $P_b^+(11130)$ and $P_b^0(11080)$, $P_b^0(11125)$, $P_b^0(11130)$, respectively.

lows [47, 54]:

$$\sigma_{\gamma p\to P^{+}_{bi}}(\sqrt{s},\Gamma_{bi}) = f_{bi}\left(\frac{\pi}{p^{*}_{\gamma}}\right)^{2} Br[P^{+}_{bi}\to\gamma p]S^{+}_{bi}(\sqrt{s},\Gamma_{bi})\Gamma_{bi},$$
$$\sigma_{\gamma n\to P^{0}_{bi}}(\sqrt{s},\Gamma_{bi}) = f_{bi}\left(\frac{\pi}{p^{*}_{\gamma}}\right)^{2} Br[P^{0}_{bi}\to\gamma n]S^{0}_{bi}(\sqrt{s},\Gamma_{bi})\Gamma_{bi}. \tag{33}$$

Here, the center-of-mass three-momentum in the incoming γN channel, p^{*}_{γ}, is defined by Eq. (18), in which one has to make the substitution $\tilde{s}\to s$ and the ratios of the spin factors f_{bi} are $f_{b1}=1$, $f_{b2}=1$, and $f_{b3}=2$.

In line with [1, 47, 55], we assume that the decays of P^{+}_{b1} and $P^{0}_{b1}(1/2)^{-}$, P^{+}_{b2} and $P^{0}_{b2}(1/2)^{-}$, and P^{+}_{b3} and $P^{0}_{b3}(3/2)^{-}$ to $\Upsilon(1S)p$ and $\Upsilon(1S)n$ are dominated by the lowest partial waves with relative orbital angular momentum $L=0$. Therefore, the branching fractions $Br[P^{+}_{bi}\to\gamma p]$ and $Br[P^{0}_{bi}\to\gamma n]$ can be expressed by adopting the vector-meson dominance model through the branching ratios $Br[P^{+}_{bi}\to\Upsilon(1S)p]$ and $Br[P^{0}_{bi}\to\Upsilon(1S)n]$, respectively, as follows [1, 47, 54, 55]:

$$Br[P^{+}_{bi}\to\gamma p] = 4\pi\alpha\left(\frac{f_{\Upsilon}}{m_{\Upsilon(1S)}}\right)^{2} f_{0,bi}\left(\frac{p^{*}_{\gamma,bi}}{p^{*}_{\Upsilon,bi}}\right) Br[P^{+}_{bi}\to\Upsilon(1S)p]$$
$$Br[P^{0}_{bi}\to\gamma n] = 4\pi\alpha\left(\frac{f_{\Upsilon}}{m_{\Upsilon(1S)}}\right)^{2} f_{0,bi}\left(\frac{p^{*}_{\gamma,bi}}{p^{*}_{\Upsilon,bi}}\right) Br[P^{0}_{bi}\to\Upsilon(1S)n] \tag{34}$$

where $f_{\Upsilon}=238$ MeV [47] is the $\Upsilon(1S)$ decay constant, $\alpha=1/137$ is the electromagnetic fine structure constant, and

$$p^{*}_{\gamma,bi} = \frac{1}{2M_{bi}}\lambda(M^{2}_{bi},0,m^{2}_{N}),\ p^{*}_{\Upsilon,bi} = \frac{1}{2M_{bi}}\lambda(M^{2}_{bi},m^{2}_{\Upsilon(1S)},m^{2}_{N}), \tag{35}$$

$$f_{0,bi} = \frac{2}{2+\gamma^{2}_{bi}},\quad \gamma^{2}_{bi} = 1+p^{*2}_{\Upsilon,bi}/m^{2}_{\Upsilon(1S)}. \tag{36}$$

Considering $Br[P^{+}_{bi}\to\Upsilon(1S)p] = Br[P^{0}_{bi}\to\Upsilon(1S)n]$ [26], we obtain the following from Eqs. (34)-(36):

$$Br[P^{0}_{bi}\to\gamma n] = Br[P^{+}_{bi}\to\gamma p]. \tag{37}$$

Using Eqs. (33) and (37), we have

$$\sigma_{\gamma p\to P^{+}_{bi}}(\sqrt{s},\Gamma_{bi}) = \sigma_{\gamma n\to P^{0}_{bi}}(\sqrt{s},\Gamma_{bi}). \tag{38}$$

Eqs. (35) and (36) yield that $(p^{*}_{\gamma,b1}, p^{*}_{\Upsilon,b1}, f_{0,b1})$ = (5.500 GeV/c, 1.223 GeV/c, 0.663), $(p^{*}_{\gamma,b2}, p^{*}_{\Upsilon,b2}, f_{0,b2})$ = (5.523 GeV/c, 1.271 GeV/c, 0.663), and $(p^{*}_{\gamma,b3}, p^{*}_{\Upsilon,b3}, f_{0,b3})$ = (5.526 GeV/c, 1.277 GeV/c, 0.663). Therefore, from Eq. (34), we obtain

$$Br[P^{+}_{b1}\to\gamma p] = 1.73\cdot10^{-4}Br[P^{+}_{b1}\to\Upsilon(1S)p],$$
$$Br[P^{+}_{b2}\to\gamma p] = 1.67\cdot10^{-4}Br[P^{+}_{b2}\to\Upsilon(1S)p],$$
$$Br[P^{+}_{b3}\to\gamma p] = 1.67\cdot10^{-4}Br[P^{+}_{b3}\to\Upsilon(1S)p]. \tag{39}$$

The free total cross sections $\sigma_{\gamma p\to P^{+}_{bi}\to\Upsilon(1S)p}(\sqrt{s},\Gamma_{bi})$ and $\sigma_{\gamma n\to P^{0}_{bi}\to\Upsilon(1S)n}(\sqrt{s},\Gamma_{bi})$ for resonant $\Upsilon(1S)$ production in the two-step processes (25)-(28) can be represented in the following forms [1, 4]:

$$\sigma_{\gamma p\to P^{+}_{bi}\to\Upsilon(1S)p}(\sqrt{s},\Gamma_{bi}) = \sigma_{\gamma p\to P^{+}_{bi}}(\sqrt{s},\Gamma_{bi})\,\theta[\sqrt{s}-(m_{\Upsilon(1S)}+m_{N})]Br[P^{+}_{bi}\to\Upsilon(1S)p], \tag{40}$$

$$\sigma_{\gamma n\to P^{0}_{bi}\to\Upsilon(1S)n}(\sqrt{s},\Gamma_{bi}) = \sigma_{\gamma n\to P^{0}_{bi}}(\sqrt{s},\Gamma_{bi})\,\theta[\sqrt{s}-(m_{\Upsilon(1S)}+m_{N})]Br[P^{0}_{bi}\to\Upsilon(1S)n]. \tag{41}$$

Here, $\theta(x)$ is the usual step function. According to Eqs. (33), (34), and (38), these cross sections are equal to each other and proportional to $Br^{2}[P^{+}_{bi}\to\Upsilon(1S)p]$ and $Br^{2}[P^{0}_{bi}\to\Upsilon(1S)n]$, respectively.

According to [1, 4], we obtain the following expression for the total cross section for $\Upsilon(1S)$ production in the γA interactions from the chains (25)-(28):

$$\sigma^{(\mathrm{sec})}_{\gamma A\to\Upsilon(1S)X}(E_{\gamma}) = \sum_{i=1}^{3}\left[\sigma^{(\mathrm{sec})}_{\gamma A\to P^{+}_{bi}\to\Upsilon(1S)p}(E_{\gamma}) + \sigma^{(\mathrm{sec})}_{\gamma A\to P^{0}_{bi}\to\Upsilon(1S)n}(E_{\gamma})\right], \tag{42}$$

where

$$\sigma^{(\mathrm{sec})}_{\gamma A\to P^{+}_{bi}\to\Upsilon(1S)p}(E_{\gamma}) = \left(\frac{Z}{A}\right) I_{V}[A,\sigma^{\mathrm{eff}}_{P_{bi}N}]\left\langle\sigma_{\gamma p\to P^{+}_{bi}}(E_{\gamma})\right\rangle_{A} \times Br[P^{+}_{bi}\to\Upsilon(1S)p],$$
$$\sigma^{(\mathrm{sec})}_{\gamma A\to P^{0}_{bi}\to\Upsilon(1S)n}(E_{\gamma}) = \left(\frac{N}{A}\right) I_{V}[A,\sigma^{\mathrm{eff}}_{P_{bi}N}]\left\langle\sigma_{\gamma n\to P^{0}_{bi}}(E_{\gamma})\right\rangle_{A} \times Br[P^{0}_{bi}\to\Upsilon(1S)n], \tag{43}$$

and

$$\left\langle\sigma_{\gamma n\to P^{0}_{bi}}(E_{\gamma})\right\rangle_{A} = \left\langle\sigma_{\gamma p\to P^{+}_{bi}}(E_{\gamma})\right\rangle_{A} = \iint P_{A}(\mathbf{p}_{t},E)\mathrm{d}\mathbf{p}_{t}\mathrm{d}E\sigma_{\gamma p\to P^{+}_{bi}}(\sqrt{s_{\Upsilon(1S)}},\Gamma^{bi}_{\mathrm{med}}) \times\theta[\sqrt{s_{\Upsilon(1S)}}-(m_{\Upsilon(1S)}+m_{N})]. \tag{44}$$

Here, $\sigma_{\gamma p\to P^{+}_{bi}}(\sqrt{s_{\Upsilon(1S)}},\Gamma^{bi}_{\mathrm{med}})$ is the "in-medium" cross section for the P^{+}_{bi} resonance production in the γp collisions (25) and Z and N are the numbers of protons and neutrons in the target nucleus. As expressed in Eq. (29), we assume that this cross section is equivalent to the free cross section of Eq. (33), in which the vacuum decay width Γ_{bi} is replaced by the in-medium width $\Gamma^{bi}_{\mathrm{med}}$, as expressed by Eqs. (30)-(32), and the vacuum center-of-mass energy squared s, presented by formula (8), is replaced by the in-medium expression (6). The term $I_{V}[A,\sigma^{\mathrm{eff}}_{P_{bi}N}]$ in Eq. (43) is defined by Eq. (4), in which one needs to make the substitution $\sigma\to\sigma^{\mathrm{eff}}_{P_{bi}N}$. Here, $\sigma^{\mathrm{eff}}_{P_{bi}N}$ is the P^{+}_{bi}, P^{0}_{bi}–nucleon effective absorption cross section. This cross section can be represented [1, 4] as a sum of the inelastic cross section $\sigma_{P_{bi}N}$, introduced earlier, and an addition to

this effective P^+_{bi}, P^0_{bi} absorption cross section, associated with their decays in the nucleus. From the standpoint of generality, we assume that the cross section $\sigma^{\rm eff}_{P_{bi}N}$ has the same value of 37 mb as was adopted in Ref. [1] for the P^+_{ci}–nucleon effective absorption cross section $\sigma^{\rm eff}_{P_{ci}N}$.

3 Numerical results and discussion

The free elementary nonresonant $\Upsilon(1S)$ production cross section in the reaction $\gamma p \to \Upsilon(1S)p$, determined based on Eqs. (22) (left panel) and (10)-(20) (right panel), and the combined (nonresonant plus resonant (40)) total cross sections are depicted in Fig. 3. From this figure, one can see that the $P^+_b(11080)$ state appears as a clear narrow independent peak at $E_\gamma = 64.95$ GeV in the combined cross section, whereas the $P^+_b(11125)$ and $P^+_b(11130)$ resonances are exhibited as one distinct wide peak at $E_\gamma \approx 65.50$ GeV, owing to the small distance between their centroids (60 MeV), for the two adopted choices (10)-(20) and (22) for the background contribution when $Br[P^+_{bi} \to \Upsilon(1S)p]$= 2%, 3%, 5%, and 10% ($i$ = 1, 2, 3). In these cases, at laboratory photon energies around the peak energies, the resonant contributions are significantly larger than the nonresonant ones. Therefore, the background reaction does not impact the direct observation of the hidden-bottom pentaquark production at these energies. The peak values of the combined cross section reach tens and hundreds of picobarns when $Br[P^+_{bi} \to \Upsilon(1S)p] = 2\%$ and 10%, respectively (it should be pointed out that the peak strengths of the combined cross section of the reaction $\gamma p \to \Upsilon(1S)p$, corresponding to the $P^+_b(11080)$ and $P^+_b(11125)$ states and obtained within the dipole Pomeron model in Ref. [27], are about of 3 and 8 nb, respectively. These are much larger than those determined in the present work). However, they are significantly smaller than that of a few nanobarns for the reaction $\gamma p \to J/\psi p$ with P^+_{ci} production [1]. This requires both extremely high luminosities, which will be accessible at future facilities such as the proposed electron–ion colliders EIC [28-30] and EicC [31, 32] in the US and China, and large-acceptance detectors. The strengths of these two peaks, obtained for $Br[P^+_{bi} \to \Upsilon(1S)p]$= 1%, decrease, particularly in comparison with the abovementioned cases, and have peak values of approximately 2 and 5 pb and 12 and 15 pb for background contribution in the form of Eqs. (22) and (10)-(20), respectively. However, in the former case, the P^+_b signal to background ratio is larger than that in the latter case by approximately one order of magnitude. Therefore, it is natural to expect that this signal can be distinguished from the background reaction as well if it has a cross section of approximately 1 pb in the energy region around the energies $E_\gamma = 64.95$ and $E_\gamma = 65.50$ GeV. To experimentally observe such a two-peak structure in the combined total cross section of the reaction $\gamma p \to \Upsilon(1S)p$, it is sufficient to have a photon energy resolution and energy binning on the order of 20–30 MeV (it should be noticed that, for example, in the GlueX experiment [5] the E_γ resolution was 20 MeV for a 10 GeV photon). Thus, the c.m. energy ranges $M_{bi} - \Gamma_{bi}/2 < \sqrt{s} < M_{bi} + \Gamma_{bi}/2$ (i = 1, 2) correspond to the laboratory photon energy regions of 64.894 GeV $< E_\gamma <$ 65.010 GeV and 65.362 GeV $< E_\gamma <$ 65.607 GeV, i.e.,ΔE_γ = 116 and 245 MeV for $P^+_b(11080)$ and $P^+_b(11125)$, respectively. This implies that to resolve the two peaks in Fig. 3, a photon energy resolution and energy bin size on the order of 20-30 MeV are required. Finally, it is worth noting that the measurement of elastic bottomonium production on protons close to threshold at electron-ion colliders facilitates the determination of the contribution of the so-called trace anomaly term to the proton mass as well [56]. This term has not yet been determined experimentally or through lattice QCD calculations [56]. The determination of this contribution would enable us to better understand the origin of the total mass of the nucleon in terms of its constituents (quarks and gluons). In addition, the use of bottomonium production at large W should also shed light on the contribution of the total gluon angular momentum to the proton spin [56].

Figure 4 displays the energy dependences of the total P^+_{b1}, P^+_{b2}, P^+_{b3} and P^0_{b1}, P^0_{b2}, P^0_{b3} production cross sections in γ^{12}C and γ^{208}Pb reactions as well as of the total P^+_{b1}, P^0_{b1} creation in γ^{12}C collisions. They are calculated based on Eqs. (42) and (43)[1)] in the scenarios with free and in-medium P^+_{bi} and P^0_{bi} spectral functions for the branching ratios $Br[P^+_{bi} \to \Upsilon(1S)p] = Br[P^0_{bi} \to \Upsilon(1S)n]$ = 1% (i = 1, 2, 3). It is seen that the hidden-bottom pentaquark resonance formation is smeared out by the Fermi motion of intranuclear nucleons. It is substantially enhanced for the in-medium case at all photon c.m.s. energies considered. The contribution to the $\Upsilon(1S)$ production on nuclei, which is attributed to the intermediate $P^+_b(11080)$ and $P^0_b(11080)$ states, amounts to approximately 25%, both at subthreshold incident energies ($W < 10.4$ GeV) and above threshold beam energies ($W > 10.4$ GeV).

The excitation functions for the nonresonant production of $\Upsilon(1S)$ mesons as well as for their resonant production via P^+_{b1}, P^+_{b2}, P^+_{b3} and P^0_{b1}, P^0_{b2}, P^0_{b3} resonance formation and decay in γ^{12}C and γ^{208}Pb collisions are presented in Figs. 5 and 6, respectively. The former are calculated using Eq. (3) for the two options employed, (10)-(20) and (22), for the nonresonant elementary cross

1) By assuming that in Eq. (43) $Br[P^+_{bi} \to \Upsilon(1S)p] = Br[P^0_{bi} \to \Upsilon(1S)n] = 1$ for all i considered.

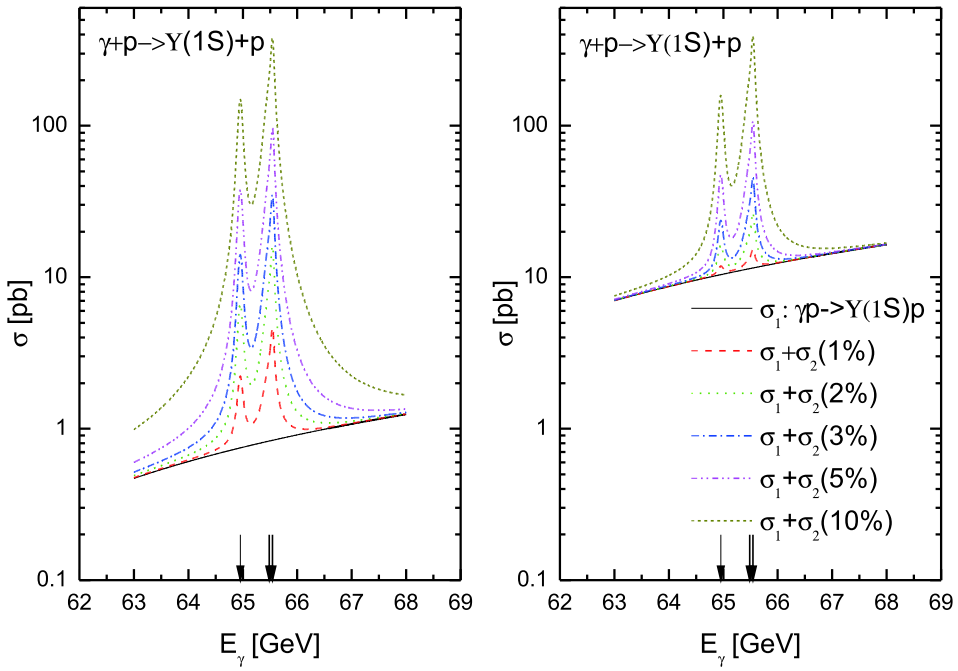

Fig. 3. (color online) Nonresonant total cross section for reaction $\gamma p \to \Upsilon(1S)p$ (solid curves), calculated based on Eqs. (22) (left panel) and (10)-(20) (right panel). Incoherent sum of it and total cross section for resonant $\Upsilon(1S)$ production in processes $\gamma p \to P_{bi}^{+} \to \Upsilon(1S)p (i = 1, 2, 3)$ calculated assuming that resonances P_{b1}^{+}, P_{b2}^{+}, and P_{b3}^{+} with spin-parity quantum numbers $J^P = (1/2)^-$, $J^P = (1/2)^-$, and $J^P = (3/2)^-$ decay to $\Upsilon(1S)p$ with lower allowed relative orbital angular momentum $L = 0$ with all three branching fractions $Br[P_{bi}^{+} \to \Upsilon(1S)p] = 1\%$, 2%, 3%, 5%, and 10% (respectively, dashed, dotted, dashed-dotted, dashed-dotted-dotted, and short-dashed curves) as functions of laboratory photon energy E_γ. Three arrows indicate resonant energies $E_\gamma^{\mathrm{R1}} = 64.952$ GeV, $E_\gamma^{\mathrm{R2}} = 65.484$ GeV, and $E_\gamma^{\mathrm{R3}} = 65.544$ GeV.

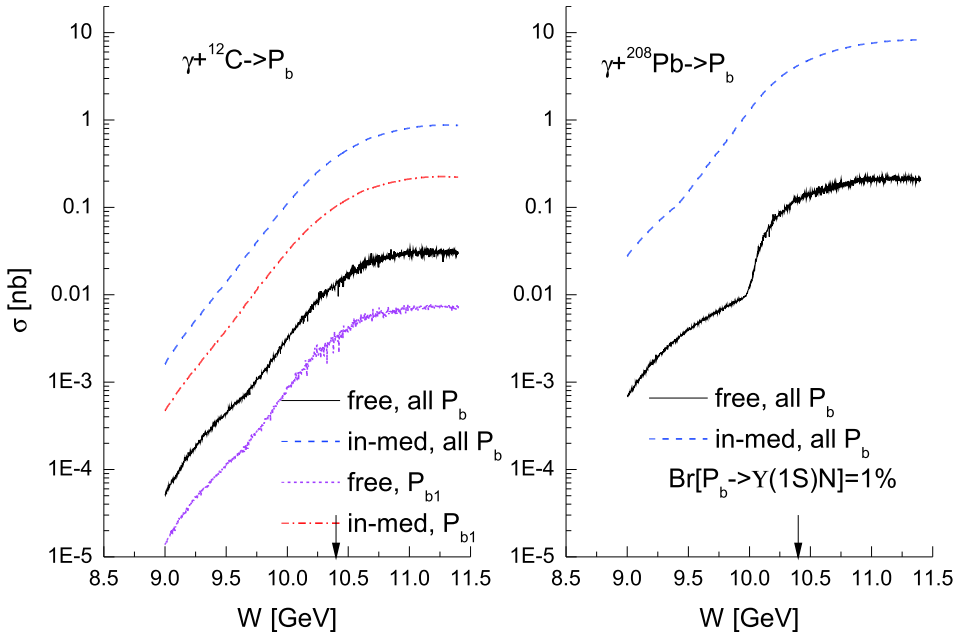

Fig. 4. (color online) Excitation functions for resonant production of P_{bi}^{+} and P_{bi}^{0} (i = 1, 2, 3) states off ^{12}C and ^{208}Pb from processes $\gamma p \to P_{bi}^{+}$ and $\gamma n \to P_{bi}^{0}$, respectively, going on off-shell target nucleons, calculated for $Br[P_{bi}^{+} \to \Upsilon(1S)p] = Br[P_{bi}^{0} \to \Upsilon(1S)n]$ = 1% for all i adopting free (solid curves) and in-medium (dashed curves) P_{bi}^{+}, P_{bi}^{0} spectral functions. ^{12}C case: Same as above, but only for processes $\gamma p \to P_{b1}^{+}$ and $\gamma n \to P_{b1}^{0}$, employing free (short-dashed) and in-medium (dotted-dashed) P_{b1}^{+} and P_{b1}^{0} spectral functions. Arrows indicate the threshold center-of-mass energy for direct $\Upsilon(1S)$ photoproduction on a free target nucleon at rest.

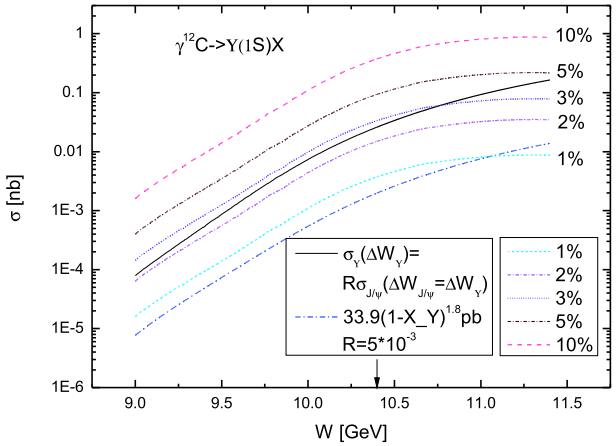

Fig. 5. (color online) Excitation functions for nonresonant and resonant production of $\Upsilon(1S)$ mesons off ^{12}C from direct $\gamma N \to \Upsilon(1S)N$ and resonant $\gamma p \to P_{bi}^{+} \to \Upsilon(1S)p$ and $\gamma n \to P_{bi}^{0} \to \Upsilon(1S)n$ (i = 1, 2, 3) reactions going on off-shell target nucleons. Curves (solid and dotted-dashed), corresponding to nonresonant production of $\Upsilon(1S)$ mesons, are calculated using Eq. (3) with elementary cross section $\sigma_{\gamma p\to\Upsilon(1S)p}$ in forms of Eqs. (10)-(20) and (22), respectively. Curves, belonging to their resonant production, are calculated using Eq. (42) for branching ratios $Br[P_{bi}^{+} \to \Upsilon(1S)p] = Br[P_{bi}^{0} \to \Upsilon(1S)n] = 1\%$, 2%, 3%, 5%, and 10% for all $i$adopting in-mediumP_{bi}^{+}, P_{bi}^{0} spectral functions. The arrow indicates the threshold center-of-mass energy for direct $\Upsilon(1S)$ photoproduction on a free target nucleon at rest.

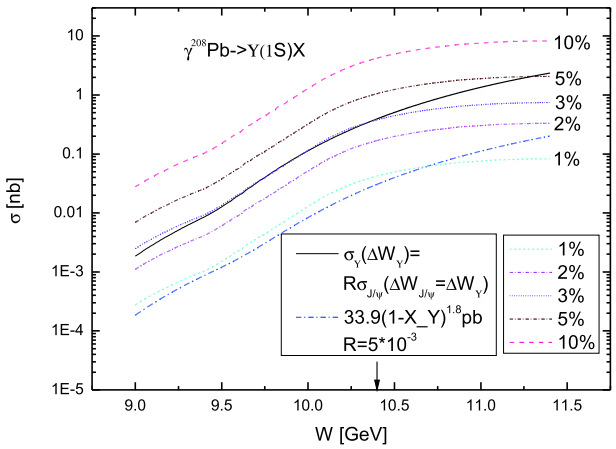

Fig. 6. (color online) Same as in Fig. 5, but for ^{208}Pb target nucleus.

section $\sigma_{\gamma p\to\Upsilon(1S)p}$, whereas the latter are determined using Eqs. (42) and (43) in the in-medium P_{bi}^{+} and P_{bi}^{0} spectral functions scenario and assuming that for all i branching ratios, $Br[P_{bi}^{+} \to \Upsilon(1S)p] = Br[P_{bi}^{0} \to \Upsilon(1S)n] = 1\%$, 2%, 3%, 5%, and 10%. One can see that the nonresonant $\Upsilon(1S)$ yield as well as that from the production and decay of the intermediate P_{bi}^{+} and P_{bi}^{0} resonances are comparable for both the considered target nuclei when $Br[P_{bi}^{+} \to \Upsilon(1S)p] = Br[P_{bi}^{0} \to \Upsilon(1S)n] = 1\%$ and 3% and when the background cross section $\sigma_{\gamma p\to\Upsilon(1S)p}$is used in the forms (22) and (10)-(20), respectively. However, if these branching ratios are higher than 1% and 3%, respectively, the resonant $\Upsilon(1S)$ production cross section will be much larger, particularly at subthreshold beam energies, than the nonresonant one and their relative strength is governed by the ratios.

Thus, the presence of the P_{bi}^{+} and P_{bi}^{0} pentaquark states leads to additional (and essential) enhancement in the behavior of the total $\Upsilon(1S)$ production cross section on nuclei both below and above threshold, and the strength of this enhancement is strongly determined by the branching fractions in their decays to the $\Upsilon(1S)p$ and $\Upsilon(1S)n$ final states, respectively. These fractions can be accurately studied experimentally at electron-ion colliders through the bottomonium excitation function measurements on nuclear targets near the threshold as well as the comparison of their results with the calculations based on the present model with known total cross sections of the direct processes (1) and (2).[1)] The collected statistics in these measurements, particularly on heavy target nuclei and at above-threshold energies, at which the resonant $\Upsilon(1S)$ production cross section reaches the values ~1-10 nb for the abovementioned branching fractions ~5%-10%, are expected to be substantially higher than what could be achieved in measurements on the nucleon target (compare Figs. 5, 6, and 3). This should enable a more accurate determination of these fractions in the measurements on nuclear targets.

4 Summary

In this study, we calculated the absolute excitation functions for the nonresonant and resonant photoproduction of $\Upsilon(1S)$ mesons off protons at threshold incident photon laboratory energies of 63-68 GeV by accounting for direct ($\gamma p \to \Upsilon(1S)p$) and two-step ($\gamma p \to P_b^{+}(11080) \to \Upsilon(1S)p, \gamma p \to P_b^{+}(11125) \to \Upsilon(1S)p,$ and $\gamma p \to P_b^{+}(11130) \to \Upsilon(1S)p$) $\Upsilon(1S)$ production channels within different scenarios for the nonresonant total cross section of the elementary reaction $\gamma p \to \Upsilon(1S)p$ and for the branching ratios of the decays $P_b^{+}(11080) \to \Upsilon(1S)p$, $P_b^{+}(11125) \to \Upsilon(1S)p$, and $P_b^{+}(11130) \to \Upsilon(1S)p$. Furthermore, an analogous function for photoproduction of $\Upsilon(1S)$ mesons on ^{12}C and ^{208}Pb target nuclei in the near-threshold center-of-

1) If these cross sections are different, then in Eq. (3) one needs to perform the following substitution $\left\langle \sigma_{\gamma p\to\Upsilon(1S)p}(E_\gamma)\right\rangle_A \to (Z/A)\left\langle \sigma_{\gamma p\to\Upsilon(1S)p}(E_\gamma)\right\rangle_A + (N/A)\left\langle \sigma_{\gamma n\to\Upsilon(1S)n}(E_\gamma)\right\rangle_A$.

mass beam energy region of 9.0-11.4 GeV was calculated by considering incoherent direct ($\gamma N \to \Upsilon(1S)N$) and two-step ($\gamma p \to P_b^+(11080) \to \Upsilon(1S)p$, $\gamma p \to P_b^+(11125) \to \Upsilon(1S)p$, $\gamma p \to P_b^+(11130) \to \Upsilon(1S)p$ and $\gamma n \to P_b^0(11080) \to \Upsilon(1S)n$, $\gamma n \to P_b^0(11125) \to \Upsilon(1S)n$, $\gamma n \to P_b^0(11130) \to \Upsilon(1S)n$) $\Upsilon(1S)$ production processes using a nuclear spectral function approach. We demonstrated that the $P_b^+(11080)$ state appears as a clear narrow independent peak at E_γ= 64.95 GeV in the combined (nonresonant plus resonant) cross section on a proton target, whereas the $P_b^+(11125)$ and $P_b^+(11130)$ resonances exhibit themselves here, owing to a small distance between their centroids (60 MeV), as one distinct wide peak at $E_\gamma \approx 65.50$ GeV for the two adopted options for the background contribution when $Br[P_{bi}^+ \to \Upsilon(1S)p] = 2\%$, 3%, 5%, and 10% ($i$ = 1, 2, 3). The peak values of the combined cross section reach tens and hundreds of picobarns when $Br[P_{bi}^+ \to \Upsilon(1S)p] = 2\%$ and 10%, respectively. Therefore, a detailed scan of the $\Upsilon(1S)$ total photoproduction cross section on a proton target in the near-threshold energy region in future high-precision experiments at electron-ion colliders should provide a definite result for or against the existence of the nonstrange hidden-bottom pentaquark states and clarify their decay rates.

It was also demonstrated that the presence of the P_{bi}^+ and P_{bi}^0 pentaquark states in $\Upsilon(1S)$ photoproduction on nuclei leads to additional (and essential) enhancement in the behavior of the total $\Upsilon(1S)$ production cross section on nuclei both below and above threshold, and the strength of this enhancement is strongly determined by the branching fractions of their decays to the $\Upsilon(1S)p$ and $\Upsilon(1S)n$ final states, respectively. This offers an indirect possibility of studying these fractions experimentally at future high-luminosity electron-ion colliders EIC and EicC in the US and China also through the near-threshold bottomonium excitation function measurements on nuclear targets. The collected statistics in these measurements, particularly on heavy target nuclei and at above threshold energies, at which the resonant $\Upsilon(1S)$ production cross section reaches the values ~ 1-10 nb for above branching fractions ~ 5%-10%, are expected to be substantially higher than what could be achieved in measurements on the nucleon target. This should enable a more accurate determination of these fractions in the measurements on nuclear targets.

References

1 E. Ya. Paryev, Nucl. Phys. A, **996**: 121711 (2020), arXiv:2003.00788[nucl-th]
2 R. Aaij *et al.* (LHCb Collaboration), Phys. Rev. Lett., **122**: 222001 (2019), arXiv:1904.03947[hep-ex]
3 R. Aaij *et al.* (LHCb Collaboration), Phys. Rev. Lett., **115**: 072001 (2015), arXiv:1507.03414[hep-ex]
4 E. Ya. Paryev and Yu.T. Kiselev, Nucl. Phys. A, **978**: 201 (2018), arXiv:1810.01715[nucl-th]
5 A. Ali *et al.* (The GlueX Collaboration), Phys. Rev. Lett., **123**: 072001 (2019), arXiv:1905.10811[nucl-ex]
6 X.-Y. Wang, X.-R. Chen, and J. He, Phys. Rev. D, **99**: 114007 (2019)
7 X.-Y. Wang *et al.*, Phys. Lett. B, **797**: 134862 (2019), arXiv:1906.04044[hep-ph]
8 C.-J. Xiao *et al.*, Phys. Rev. D, **100**: 014022 (2019)
9 A. Ali *et al.*, arXiv: 1907.06507[hep-ph]
10 H. X. Chen, W. Chen, and S.-L. Zhu, Phys. Rev. D, **100**: 051501 (2019), arXiv:1903.11001[hep-ph]
11 R. Chen, Z. F. Sun, X. Liu *et al.*, Phys. Rev. D, **100**: 011502 (2019), arXiv:1903.11013[hep-ph]
12 F. K. Guo, H. J. Jing, U. G. Meissner *et al.*, Phys. Rev. D, **99**: 091501 (2019), arXiv:1903.11503[hep-ph]
13 M. Z. Liu *et al.*, Phys. Rev. Lett., **122**: 242001 (2019), arXiv:1903.11560[hep-ph]
14 J. R. Zhang, arXiv: 1904.10711[hep-ph]
15 H. Huang, J. He, and J. Ping, arXiv: 1904.00221[hep-ph]
16 Y. Shimizu, Y. Yamaguchi, and M. Harada, arXiv: 1904.00587[hep-ph]
17 C. W. Xiao, J. Nieves, and E. Oset, Phys. Rev. D, **100**: 014021 (2019), arXiv:1904.01296[hep-ph]
18 L. Meng, B. Wang, G. J. Wang *et al.*, Phys. Rev. D, **100**: 014031 (2019) [arXiv: 1905.04113[hep-ph]]; J. B. Cheng and Y. R. Liu, Phys. Rev. D, **100**: 054002 (2019) [arXiv: 1905.08605[hep-ph]]
19 J. J. Wu, R. Molina, E. Oset *et al.*, Phys. Rev. Lett., **105**: 232001 (2010) [arXiv: 1007.0573[nucl-th]]
20 J. J. Wu, R. Molina, E. Oset *et al.*, Phys. Rev. C, **84**: 015202(2011) [arXiv: 1011.2399[nucl-th]]
21 W. L. Wang, F. Huang, Z. Y. Zhang *et al.*, Phys. Rev. C, **84**: 015203 (2011) [arXiv: 1101.0453[nucl-th]]
22 J. J. Wu, T.-S. H. Lee, and B. S. Zou, Phys. Rev. C, **85**: 044002 (2012) [arXiv: 1202.1036[nucl-th]]
23 Z. C. Yang, Z. F. Sun, J. He *et al.*, Chin. Phys. C, **36**: 6 (2012) [arXiv: 1105.2901[hep-ph]]
24 C. Garcia-Recio, J. Nieves, O. Romanets *et al.*, Phys. Rev. D, **87**: 074034 (2013) [arXiv: 1302.6938[hep-ph]]
25 Y. Huang, J. He, H. F. Zhang *et al.*, J. Phys. G, **41**(11): 115004 (2014) [arXiv: 1305.4434[nucl-th]]
26 T. Gutsche and V. E. Lyubovitskij, Phys. Rev. D, **100**: 094031 (2019), arXiv:1910.03984[hep-ph]
27 X.-Y. Wang, J. He, and X. Chen, arXiv: 1912.07156[hep-ph]
28 A. Accardi *et al.*, Eur. Phys. J. A, **52**: 268 (2016), arXiv:1212.1701[nucl-ex]
29 M. Lomnitz and S. Klein, Phys. Rev. C, **99**: 015203 (2019), arXiv:1803.06420[nucl-ex]
30 X. Li *et al.*, arXiv: 2002.05880[nucl-ex]
31 X. Chen, PoS DIS, **2018**: 170 (2018), arXiv:1809.00448[nucl-ex]
32 X. Chen, PoS SPIN, **2018**: 160 (2019)
33 A. Mishra and D. Pathak, Phys. Rev. C, **90**: 025201 (2014), arXiv:1404.2517[nucl-th]
34 S. V. Efremov and E. Ya. Paryev, Eur. Phys. J. A, **1**: 99 (1998)
35 E. Ya. Paryev, Eur. Phys. J. A, **7**: 127 (2000)
36 E. Ya. Paryev, Chinese Physics C, **42**(8): 084101 (2018)
37 T. Song, K. C. Han, and C. M. Ko, Phys. Rev. C, **85**: 014902 (2012), arXiv:1109.6691[nucl-th]
38 X. Du, M. He, and R. Rapp, arXiv: 1704.04838[hep-ph]
39 X. Du, S. Liu, and R. Rapp, arXiv: 1904.00113[nucl-th]
40 J. Breitweg *et al.* (ZEUS Collaboration), Phys. Lett. B, **437**: 432 (1998), arXiv:hep-ex/9807020
41 C. Adloff *et al.* (H1 Collaboration), Phys. Lett. B, **483**: 23 (2000), arXiv:hep-ex/0003020

42 S. Chekanov *et al*. (ZEUS Collaboration), Phys. Lett. B, **680**: 4 (2009), arXiv:0903.4205[hep-ex]
43 A. M. Sirunyan *et al*. (CMS Collaboration), Eur. Phys. J. C, **79**(3): 277 (2019), arXiv:1809.11080[hep-ex]
44 R. Aaij *et al*. (LHCb Collaboration), JHEP, **1509**: 084 (2015), arXiv:1505.08139[hep-ex]
45 Y. Hatta, M. Strikman, J. Xu *et al*., arXiv: 1911.11706[hep-ph]
46 S. J. Brodsky, E. Chudakov, P. Hoyer *et al*., Phys. Lett. B, **498**: 23 (2001)
47 M. Karliner and J. L. Rosner, Phys. Lett. B, **752**: 329 (2016), arXiv:1508.01496[hep-ph]
48 J. J. Wu, L. Zhao, and B. S. Zou, arXiv: 1011.5743[hep-ph]
49 C. W. Xiao and E. Oset, Eur. Phys. J. A, **49**: 139 (2013), arXiv:1305.0786[hep-ph]
50 H. Huang and J. Ping, Phys. Rev. D, **99**: 014010 (2019), arXiv:1811.04260[hep-ph]
51 J. Wu, Y. R. Liu, K. Chen *et al*., Phys. Rev. D, **95**: 034002 (2017), arXiv:1701.03873[hep-ph]
52 Y. Yamaguchi *et al*., Phys. Rev. D, **96**: 114031 (2017), arXiv:1709.00819[hep-ph]
53 B. Wang, L. Meng, and S. L. Zhu, JHEP, **1911**: 108 (2019), arXiv:1909.13054[hep-ph]
54 V. Kubarovsky and M. B. Voloshin, Phys. Rev. D, **92**: 031502 (2015), arXiv:1508.00888[hep-ph]
55 A. N. Hiller Blin *et al*., Phys. Rev. D, **94**: 034002 (2016)
56 S. Joosten and Z.-E. Meziani, arXiv: 1802.02616[hep-ex]